Journal of Applied Mechanics and Technical Physics, Vol. 44, No. 1, pp. 1–16, 2003

POINCARÉ MAPPING METHOD FOR HYDRODYNAMIC SYSTEMS. DYNAMIC CHAOS IN A FLUID LAYER BETWEEN ECCENTRICALLY ROTATING CYLINDERS

A. G. Petrov

UDC 532.5:517.928.7

Investigation of the plane–parallel motion of particles of an incompressible medium reduces to investigation of a Hamiltonian system. The Hamiltonian function is a stream function. The time-periodic mixing of an incompressible medium is described by a time-periodic Hamiltonian function. The mixing of the medium is associated with dynamic chaos. Transition to dynamic chaos is studied by analysis of the positions of Lagrangian particles at times divisible by the period — Poincaré recurrence points. The set of Poincaré recurrence points is studied with the use of Poincaré mapping on the phase flow. A method for constructing Poincaré maps in parametric form is proposed. A map is constructed as a series in a small parameter. It is shown that the parametric method has a number of advantages over the generating function method is shown. The proposed method is used to examine the motion of particles of an incompressible viscous fluid layer between two circular cylinders. The outer cylinder is immovable, and the inner cylinder rotates about a point that does not coincide with the centers of both cylinders. An optimal mode for the motion is established, in which the area of the chaotic region is maximal.

Key words*: hydrodynamic systems, Cauchy problem, small parameter, dynamic chaos.*

1. Formulation of the Problem. We consider the Cauchy problem for the Hamiltonian equations for a system with n degrees of freedom:

$$\dot{\boldsymbol{X}} = H_{\boldsymbol{Y}}, \quad \dot{\boldsymbol{Y}} = -H_{\boldsymbol{X}}, \quad \boldsymbol{X}(t_0) = \boldsymbol{X}_0, \quad \boldsymbol{Y}(t_0) = \boldsymbol{Y}_0, \quad H_{\boldsymbol{X}} = \frac{\partial H}{\partial \boldsymbol{X}}, \quad H_{\boldsymbol{Y}} = \frac{\partial H}{\partial \boldsymbol{Y}}. \tag{1.1}$$

Here $H(t, \boldsymbol{X}, \boldsymbol{Y}) = H(t+T, \boldsymbol{X}, \boldsymbol{Y})$ is an arbitrary, fairly smooth T-periodic function and $\boldsymbol{X}$ and $\boldsymbol{Y}$ are n-dimensional vectors.

At present, there is no universally accepted definition of random motions. For systems with one degree of freedom, it is possible to give a geometrically simple, though mathematically nonrigorous, definition of chaos. In this case, the Hamiltonian can be treated as a stream function for incompressible fluid flow. The Hamiltonian system (1.1) defines the motion of Lagrangian particles of a medium. Let us introduce some notions required to define chaos for Lagrangian particles.

On the trajectory $\boldsymbol{X}(t, t_0, \boldsymbol{X}_0, \boldsymbol{Y}_0)$, $\boldsymbol{Y}(t, t_0, \boldsymbol{X}_0, \boldsymbol{Y}_0)$ determined by solving system (1.1), we consider the positions of the points $\boldsymbol{X}(t_n, t_0, \boldsymbol{X}_0, \boldsymbol{Y}_0)$, $\boldsymbol{Y}(t_n, t_0, \boldsymbol{X}_0, \boldsymbol{Y}_0)$, where $t_n = t_0 + Tn$ $(n = 0, \pm 1, \pm 2, \ldots)$ at times multiple to the period. Such points are called Poincaré recurrence points (PRP).

For the plane–parallel flow of an incompressible medium there is a stream function, which will be the Hamiltonian of the system. The trajectory of a Lagrangian particle of the medium is found by solving the problem (1.1), and the PRP represents the particle track recorded at a frame rate corresponding to the period T. The PRP form a countable set of points on a plane, which, generally speaking, depends on t_0, $\boldsymbol{X}_0$, and $\boldsymbol{Y}_0$. If the set of PRP belongs

Institute of Problems of Mechanics, Russian Academy of Sciences, Moscow 117526. Translated from Prikladnaya Mekhanika i Tekhnicheskaya Fizika, Vol. 44, No. 1, pp. 3–21, January–February, 2003. Original article submitted July 8, 2002.

0021-8944/03/4401-0001 $25.00

to a one-dimensional line, this line is called an invariant curve. For ordered motion, all sets of PRP form a set of invariant curves. The type of motion in which the set of PRP fills a two-dimensional region will be called random motion of the PRP.

For a periodic dependence of the Hamiltonian on time, the set of PRP can be calculated from the recursive formulas $(\boldsymbol{X}_n, \boldsymbol{Y}_n) = P_{t_0}^T(\boldsymbol{X}_{n-1}, \boldsymbol{Y}_{n-1})$ [$P_{t_0}^{\Delta t}$ ($\Delta t = t - t_0$) is a map on the phase flow of system (1.1), i.e., a solution of problem (1.1)]. The map over the period $P_{t_0}^T$ is called the Poincaré map.

It should be noted that the above definition of random motion does not depend on t_0. Indeed, with conversion from t_0 to $t_0 + \Delta t$ ($0 < \Delta t < T$), the set of PRP is transformed by means of the continuous map $P_{t_0}^{\Delta t}$. In this case, a one-dimensional line or a two-dimensional region becomes a one-dimensional line or a two-dimensional region, respectively. If $\Delta t = kT$ is a multiple of the period, the map $P_{t_0}^{\Delta t} = P_{t_0}^{kT}$ transforms the PRP into itself. Otherwise, Δt can be represented by $\Delta t = kT + \Delta t'$ ($0 < \Delta t' < T$). The map $P_{t_0}^{\Delta t}$ is identical to the map $P_{t_0}^{\Delta t'}$ and does not change the topological structure of the PRP.

For definiteness, we choose $t_0 = 0$ and omit the superscript and subscript in the notation of the Poincaré map: $P_0^T = P$.

Investigation of the chaotic nature of motion using the Poincaré map is called the method of Poincaré sections [1–4]. Because determining Poincaré maps is a complex computational problem,the PRP are commonly found numerically, and analytical methods are used only for very simple systems.

In studies of systems with one degree of freedom with a Hamiltonian of the standard form

$$H = \varepsilon H_1 + \varepsilon^2 H_2 + \varepsilon^3 H_3 + \ldots, \tag{1.2}$$

where ε is a small parameter, the following theoretical results are used. It is known that an autonomous Hamiltonian system (the Hamiltonian does not depend explicitly on time) is integrable. Lagrangian particles lie on one-dimensional streamlines $H(\boldsymbol{X}_n, \boldsymbol{Y}_n) = \text{const}$, and the motion is ordered. For a nonautonomous system of the standard form, the asymptotic procedure of the averaging method [5, 6] allows one to construct a nearly identical canonical change of variables $\boldsymbol{X}, \boldsymbol{Y} \to \boldsymbol{X}, \boldsymbol{Y}$ for any integer $k > 0$, so that with accuracy up to ε^{k+1}, the equations in the new variables have the form of an autonomous Hamiltonian system with a Hamiltonian $\bar{H}(\boldsymbol{X}, \boldsymbol{Y})$.

It should be born in mind that the averaged Hamiltonian for any Hamiltonian system (1.1) cannot be exactly determined in principle. According to the Neishtadt theorem [7], the Hamiltonian of the system can be reduced to an almost autonomous form $\bar{H}(\boldsymbol{X}, \boldsymbol{Y}) + R(t, \boldsymbol{X}, \boldsymbol{Y})$, where $|R| < C_1 \exp(-C/\varepsilon)$, by a sequence of canonical replacements. Exact determination of the averaged autonomous Hamiltonian is possible only for integrable Hamiltonian systems. Generally, the estimate of the remainder R cannot be improved.

In the absence of an exponentially small component ($R = 0$), the system is integrable, and chaos is not observed in the case of one degree of freedom. Chaos is due to the exponentially small quantity $R(t, \boldsymbol{X}, \boldsymbol{Y})$, which cannot be determined by averaging methods. Therefore, it makes no sense to employ averaging methods in studies of transition to random motions in systems with one degree of freedom.

According to the results of asymptotic methods described above, the following typical picture of chaos growth in nonintegrable dynamic systems is observed with increase in the parameter ε. For a small ε, the sets of PRP lie on invariant curves $\bar{H}(\boldsymbol{X}_n, \boldsymbol{Y}_n) = \text{const}$, determined by averaging methods with accuracy up to $R = C_1 \exp(-C/\varepsilon)$. In this case, by virtue of the smallness of R, chaos is practically invisible. With a certain increase in ε, the exponential component begins to show up, chaos becomes noticeable, and the area of the chaotic region increases rapidly with increase in ε.

The occurrence of chaos is usually associated with the existence of unstable fixed points of the Poincaré map [1–4, 8]. The fixed point $P(\boldsymbol{X}, \boldsymbol{Y}) = (\boldsymbol{X}, \boldsymbol{Y})$ corresponds to a periodic solution with period T, and the fixed point $P^k(\boldsymbol{X}, \boldsymbol{Y}) = (\boldsymbol{X}, \boldsymbol{Y})$ to a periodic solution with period kT. The problem of Lyapunov's stability of a periodic solution reduces to solving the stability problem for the fixed point of the map using the method of Lyapunov's exponents [3]. Because the analytic form of the map P is unknown, Lyapunov's exponents are determined numerically. Below the map P and Lyapunov's exponents are found analytically in the form of series in ε.

Proving the chaotic state using any rigorous definition of chaos is an extremely difficult problem even for a system with one degree of freedom. Examples of proof of the chaotic state for simple maps are given in [9]. For Hamiltonian systems, the chaotic state is proved employing Mel'nikov's theorem [3], which involves evaluation of a rather complex integral. Analytically, by using the Mel'nikov method, it is possible to prove the chaotic nature of motion for a mathematical pendulum with a vibrating suspension point. In this system with a time-periodic

Hamiltonian there is a separatrix representable in simple analytic form, which allows use of Mel'nikov's theorem. Usually, verification of the chaotic state by means of Mel'nikov's theorem or another method is performed by rather unwieldy numerical methods.

Some fairly simple hydrodynamic systems are studied in [8] using numerical determination of PRP. The motion of a viscous fluid in a region with a time varying boundary has not been studied. The motion of particles of incompressible media with different rheology in a thin deformed layer was studied in [10]. The conditions of no tangential velocity are imposed on the boundaries. Numerical calculations showed that chaos is practically absent in such systems at small Reynolds numbers.

In the present paper, we propose a parametric method for constructing maps on the phase flow of Hamiltonian systems. The advantages of the parametric method over the well-known generating function method are shown. The main advantages are the ease and high accuracy of calculations of the Poincaré recurrence points over a wide range of parameters.

The asymptotic theory describing transition to random motion is used to study a thin layer of a high-viscosity fluid between two eccentrically rotating cylinders.

2. Equation Defining the Poincaré Map. *Generating Function Method.* The generating function method is used for canonical transformations [11, 12]. This method can also be used to construct Poincaré maps. For simplicity, we consider the Cauchy problem (1.1) for a system with one degree of freedom (although all results are easy to extend to the general case of a system with n degrees of freedom). A map $\boldsymbol{X}_0, \boldsymbol{Y}_0 \to \boldsymbol{X}, \boldsymbol{Y}$ that retains the phase volume is represented via a differentiable function of mixed variables $\boldsymbol{X}_0\boldsymbol{Y} + S(t, \boldsymbol{X}_0, \boldsymbol{Y})$ (generating function) by the relation

$$\boldsymbol{X} = \boldsymbol{X}_0 + \frac{\partial S}{\partial \boldsymbol{Y}}, \qquad \boldsymbol{Y}_0 = \boldsymbol{Y} + \frac{\partial S}{\partial \boldsymbol{X}_0}. \tag{2.1}$$

If the condition

$$1 + \frac{\partial^2 S}{\partial \boldsymbol{X}_0\, \partial \boldsymbol{Y}} > 0 \tag{2.2}$$

is satisfied, the system is solvable for $\boldsymbol{X}$ and $\boldsymbol{Y}$. The result of the solution is a map with Jacobian equal to unity for any function S. If the generating function S is determined from the Hamiltonian–Jacobi equation

$$S_t(t, \boldsymbol{X}_0, \boldsymbol{Y}) = H(t, \boldsymbol{X}_0 + S_{\boldsymbol{Y}}(t, \boldsymbol{X}_0, \boldsymbol{Y}), \boldsymbol{Y}), \tag{2.3}$$

the map (2.1) is a solution of the Hamiltonian system (1.1).

For a system of the standard form, the function S is represented as a series in powers of ε. Any finite number of terms of the series defines a map that retains the phase volume. This is an advantage of the generating function method. However, this method also has a number of significant disadvantages:

1. Maps of the form (2.1) are not universal. (For example, rotation through 90° cannot be represented in the form of (2.1). For such a map, one needs to chose another pair of variables in the generating function, but identity transformations cannot be represented in these variables [11].)

2. The resolvability condition considerably narrows the range of the parameter ε. In addition, this condition is noninvariant under rotation of Cartesian axes on the phase plane.

Below we propose a method for parametric representation of maps that is free of the indicated disadvantages.

Parametric Method. Let us seek a map $\boldsymbol{X}_0 \to \boldsymbol{X}$ with Jacobian equal to unity in parametric form $\boldsymbol{X} = \boldsymbol{X}(t, \boldsymbol{x})$, $\boldsymbol{X}_0 = \boldsymbol{X}(t, \boldsymbol{x})$, where $\boldsymbol{x}$, $\boldsymbol{X}_0$, and $\boldsymbol{X}$ are two-dimensional vectors, $\boldsymbol{X}_0 = \boldsymbol{X}(0)$ is the initial point on the trajectory, $\boldsymbol{X}$ is a point on the trajectory at time t, and $\boldsymbol{x}$ is a certain vector parameter. Any such map can be represented as

$$\boldsymbol{X}_0 = \boldsymbol{x} - \frac{1}{2}\, I\, \frac{\partial \Psi}{\partial \boldsymbol{x}}, \qquad \boldsymbol{X} = \boldsymbol{x} + \frac{1}{2}\, I\, \frac{\partial \Psi}{\partial \boldsymbol{x}}, \qquad \frac{\partial \Psi}{\partial \boldsymbol{x}} = \begin{pmatrix} \Psi_x \\ \Psi_y \end{pmatrix}, \tag{2.4}$$

where $\Psi(t, \boldsymbol{x})$ is an arbitrary function of the vector-parameter and time and I is a symplectic matrix,

$$\boldsymbol{X} = \begin{pmatrix} X \\ Y \end{pmatrix}, \qquad \boldsymbol{x} = \begin{pmatrix} x \\ y \end{pmatrix}, \qquad I = \begin{pmatrix} 0 & 1 \\ -1 & 0 \end{pmatrix}. \tag{2.5}$$

The Jacobians of both maps (2.4) are equal to the same function:

$$J(t, \boldsymbol{x}) = \det\Big(\frac{\partial \boldsymbol{X}}{\partial \boldsymbol{x}}\Big) = \det\Big(\frac{\partial \boldsymbol{X}_0}{\partial \boldsymbol{x}}\Big) = 1 + \frac{1}{4}\, \det\Big(\frac{\partial^2 \Psi}{\partial \boldsymbol{x}\, \partial \boldsymbol{x}}\Big). \tag{2.6}$$

Therefore, the Jacobian of the superposition of maps $\boldsymbol{X}_0 \to \boldsymbol{x} \to \boldsymbol{X}$ is identically equal to unity. The map (2.4) is an analog of (2.1), and the condition (2.2) is replaced by the condition $J > 0$.

In order that the map (2.5) be a solution of the Cauchy problem for the Hamiltonian equations, the function Ψ should satisfy the analog of the Hamiltonian–Jacobi equation (2.3)

$$\frac{\partial \Psi}{\partial t} = H\Big(t, \boldsymbol{x} + \frac{1}{2}\, I\, \frac{\partial \Psi}{\partial \boldsymbol{x}}\Big), \qquad \Psi(t_0, \boldsymbol{x}) = 0. \tag{2.7}$$

The map (2.4) on a plane is written in coordinate form as

$$X_0 = x - \Psi_y/2, \quad Y_0 = y + \Psi_x/2, \qquad X = x + \Psi_y/2, \quad Y = y - \Psi_x/2. \tag{2.8}$$

Such a parametric form of a map with Jacobian equal to unity is obtained in [13].

According to (2.8), Eq. (2.7) for the function $\Psi(t, x, y)$ is written as

$$\frac{\partial \Psi}{\partial t} = H\Big(t, x + \frac{1}{2}\, \frac{\partial \Psi}{\partial y}, y - \frac{1}{2}\, \frac{\partial \Psi}{\partial y}\Big), \qquad \Psi(0, x, y) = 0.$$

The results given above underly the asymptotic method of obtaining Poincaré maps. Let us formulate them as the following theorem.

Theorem 1. *The map* (2.4) *is a solution of the problem* (1.1) *if and only if the function* Ψ *is a solution of the problem* (2.7).

Theorem 1 is a special case of the more general theorem on parametrization of canonical transformations, which is proved below.

3. Parametric Form of Canonical Transformations. The general result of parametrization of the canonical change of variables in Hamiltonian systems is formulated as the following theorem.

Theorem 2. *Let a transformation of variables* $q, p \to Q, P$ *be written in parametric form*

$$q = x - \Psi_y/2, \quad p = y + \Psi_x/2, \qquad Q = x + \Psi_y/2, \quad P = y - \Psi_x/2. \tag{3.1}$$

Then,

1) *the Jacobians of the two transformations* $q = q(t, x, y)$, $p = p(t, x, y)$ *and* $Q = Q(t, x, y)$, $P = P(t, x, y)$ *are identically equal:*

$$\frac{\partial(q, p)}{\partial(x, y)} = \frac{\partial(Q, P)}{\partial(x, y)} = J(t, x, y);$$

2) *for* $J > 0$, *the transformation* (3.1) *of variables* $q, p \to Q, P$ *is canonical and transform a Hamiltonian system* $\tilde{H} = \tilde{H}(t, q, p)$ *into a Hamiltonian system* $H = H(t, Q, P)$ *if the function* Ψ *is a solution of the equation*

$$\Psi_t(t, x, y) + \tilde{H}(t, q, p) = H(t, Q, P), \tag{3.2}$$

where the arguments q, p *and* Q, P *in the Hamiltonians* H *and* $\tilde{H}$ *are expressed in terms of the parameters* x *and* y *by* (3.1).

We shall prove ststement 2 using the canonicity criterion, according to which the differential form $\delta F = P\delta Q - p\delta q - (\tilde{H} - H)\delta t$ is a full differential of a certain function $\delta F(t, x, y) = F_t \delta t + F_x \delta x + F_y \delta y$ [11].

Substituting expressions (3.1) of the variables q, p, Q, and P in terms of the parameters x and y into the differential form δF, replacing $H - \tilde{H}$ by Ψ_t according to (3.2), and performing obvious transformations, we obtain

$$\delta F = (y - \Psi_x/2)(\delta x + \Psi_{yt}\delta t/2 + \Psi_{yx}\delta x/2 + \Psi_{yy}\delta y/2)$$

$$- (y + \Psi_x/2)(\delta x - \Psi_{yt}\delta t/2 - \Psi_{yx}\delta x/2 - \Psi_{yy}\delta y/2) - \Psi_t \delta t$$

$$= y(\Psi_{yt}\delta t + \Psi_{yx}\delta x + \Psi_{yy}\delta y) - \Psi_x \delta x - \Psi_t \delta t = \delta(y\Psi_y - \Psi)$$

as was to be proved.

Statement 1 follows from the fact that for the canonical replacement, the Jacobian $\partial(\boldsymbol{Q}, \boldsymbol{P})/\partial(\boldsymbol{q}, \boldsymbol{p}) = 1$. Here $\boldsymbol{q}$, $\boldsymbol{p}$, $\boldsymbol{Q}$, $\boldsymbol{P}$, $\boldsymbol{x}$, and $\boldsymbol{y}$ are n-dimensional vectors. Therefore, the method of canonical replacements described above is valid for Hamiltonian systems of an arbitrary order n.

In the particular case of $\tilde{H} = 0$, the variables $\boldsymbol{q}$ and $\boldsymbol{p}$ are the initial point $\boldsymbol{q} = \boldsymbol{X}_0$, $\boldsymbol{p} = \boldsymbol{Y}_0$ of the trajectory $Q = X(t)$, $P = Y(t)$ of a system with a Hamiltonian $H(t, X, Y)$. Thus, Theorem 1 is also proved.

4. Asymptotic Method for Constructing Poincaré Maps. Let the Hamiltonian has a small factor ε (system of the standard form) and is represented as the power series (1.2). Then, the solution of Eq. (2.7) with zeroth initial conditions is represented as a series in powers of ε:

$$\Psi = \varepsilon\Psi_1 + \varepsilon^2\Psi_2 + \varepsilon^3\Psi_3 + \dots \ . \tag{4.1}$$

To calculate the coefficients of the series, we substitute the series (4.1) into the right side of Eq. (2.7). Let us expand the right side in a power series of ε:

$$H(t, x + \Psi_{y,y}/2 - \Psi_x/2, \varepsilon) = \varepsilon H_1 + \varepsilon^2(H_2 + H_{1x}\Psi_{1y}/2 - H_{1y}\Psi_{1x}/2)$$

$$+ \varepsilon^3[H_3 + (H_{2x}\Psi_{1y} - H_{2y}\Psi_{1x} + H_{1x}\Psi_{2y} - H_{1y}\Psi_{2x})/2$$

$$+ (H_{1xx}\Psi_{1y}^2 - 2H_{1xy}\Psi_{1x}\Psi_{1y} + H_{1yy}\Psi_{1x}^2)/8] + \dots \ .$$

For the derivatives of Ψ_n, we have

$$\frac{\partial\Psi_1}{\partial t} = H_1, \qquad \frac{\partial\Psi_2}{\partial t} = H_2 + \frac{1}{2}(H_{1x}\Psi_{1y} - H_{1y}\Psi_{1x}),$$

$$\frac{\partial\Psi_3}{\partial t} = H_3 + \frac{1}{2}(H_{2x}\Psi_{1y} - H_{2y}\Psi_{1x} + H_{1x}\Psi_{2y} - H_{1y}\Psi_{2x}) + \frac{1}{8}(H_{1xx}\Psi_{1y}^2 - 2H_{1xy}\Psi_{1x}\Psi_{1y} + H_{1yy}\Psi_{1x}^2), \dots \ .$$

From this, the coefficients of series (4.1) are expressed in terms of the coefficients of series (1.2) by integration over t taking into account the conditions $\Psi_n = 0$ at $t = 0$. For the Poincaré map over period T with accuracy to third order, we obtain

$$\Psi = \int_0^T \Big[\varepsilon H_1(t, x, y) + \varepsilon^2\Big(H_2(t, x, y) - \frac{1}{2}\Big\{H_1(t, x, y), \int_0^t H_1(t', x, y)\, dt'\Big\}\Big)\Big]\, dt, \tag{4.2}$$

where $\{f, h\} = f_y h_x - f_x h_y$ is the Poisson's bracket.

The convergence of series (4.2) is proved by the majorant method in the same manner as for the general system of differential equations in standard form [14]. Thus, the Poincaré map is an analytic function in the parameter ε, which agrees with the well-known theorem on the analyticity of solutions of differential equations in parameter.

Autonomous Hamiltonian Systems. For an autonomous Hamiltonian system with a Hamiltonian $H(X, Y)$, the procedure of expanding in a power series of the function Ψ is considerably simplified. The solution of Eq. (2.7) $\Psi(t, x, y)$ is an odd function in the argument t [15]. This property can be used to simplify calculations of the series of the function Ψ in the case of a Hamiltonian of the standard form $H = \varepsilon H_1 + \varepsilon^2 H_2 + \varepsilon^3 H_3 + \dots$. The Hamiltonian is formally written as $H = \varepsilon\tilde{H}(X, Y, \varepsilon_1)$, where $\tilde{H} = H_1 + \varepsilon_1 H_2 + \varepsilon_1^2 H_3 + \dots$. For $\varepsilon_1 = \varepsilon$, this Hamiltonian coincides with the initial one. By virtue of the indicated property, the solution of (2.7) for $\varepsilon_1 = \text{const}$ is represented as a series in odd powers of εt:

$$\Psi = (\varepsilon t)\tilde{\Psi}_1 + (\varepsilon t)^3\tilde{\Psi}_3 + (\varepsilon t)^5\tilde{\Psi}_5 + \dots \ .$$

The coefficients of this series $\tilde{\Psi}_n(x, y, \varepsilon_1)$ are much easier to calculate from Eq. (2.7) than in the general case. Thus, to obtain the series with accuracy up to $(\varepsilon t)^5$, it is necessary to calculate only two coefficients rather than four, as in the general case:

$$\Psi = (\varepsilon t)\tilde{H}(x, y, \varepsilon_1) + (\varepsilon t)^3[\tilde{H}_{xx}\tilde{H}_y^2 - 2\tilde{H}_{xy}\tilde{H}_x\tilde{H}_y + \tilde{H}_{yy}\tilde{H}_x^2]/8 + O(\varepsilon t)^5. \tag{4.3}$$

To obtain the final series in powers if ε, it is necessary to set $\varepsilon = \varepsilon_1$ and to substitute the series $\tilde{H}(X, Y, \varepsilon) = H_1 + \varepsilon H_2 + \varepsilon^2 H_3 + \dots$ into (4.3).

Because a nonautonomous Hamiltonian system can be reduced to an autonomous system by increasing the number of degree of freedom by unity, the procedure of deriving the Poincaré map for a general nonautonomous system can be reduced to the procedure described above for autonomous systems. The significant simplifications for autonomous systems can be used to obtain a power series with a larger number of terms by less unwieldy calculations. Thus, using an analog of the formula (4.3), we obtain a map that is two orders of magnitude (in ε) more accurate than formulas (4.2).

Averaging Procedure. An averaging procedure using generating functions is described in [5]. The parametric method is also an effective means for constructing averaged Hamiltonian in the case of a time-periodic Hamiltonian. Examples of such calculations accurate up to ε^3 are given in [10, 15, 16].

The averaged Hamiltonian multiplied by the period T and the mapping function coincide with accuracy up to ε^3:

$$T\bar{H}(X,Y,\varepsilon) = \Psi(T,X,Y,\varepsilon). \tag{4.4}$$

(For the generating function there is no such a simple expression in this approximation.) Taking into account (4.2), from (4.4) we obtain the well-known formula of the averaged Hamiltonian in this approximation [5]:

$$\bar{H} = \frac{1}{T}\,\bar{\Psi} = \Big\langle H - \frac{1}{2}\Big\{H, \int\limits_0^t H\,dt\Big\}\Big\rangle + O(\varepsilon^3)$$

(the expression in angular brackets denotes the average over the period).

Similar simplifications can be carried out in the higher Approximations as well.

Thus, to calculate the coefficients of asymptotic expansions of the averaged Hamiltonian, the parametric method is more effective than the generating function method [5].

5. Map of a Small Region. We assume that the Hamiltonian $H(t,X,Y,\varepsilon)$ is an analytic function of the coordinates X and Y, time t, and the parameter ε. As a function of time, the Hamiltonian has period T. The coordinates $X(t)$ and $Y(t)$ vary in a certain compact region.

According to the theory of finite strains [17], the map of a small neighborhood of a point $\boldsymbol{X}_0$ is given by the matrix $A = \partial\boldsymbol{X}/\partial\boldsymbol{X}_0$ ($\boldsymbol{X}$ is the radius-vector with the coordinates X and Y). Using the map (2.7), we can express the matrix A in terms of derivatives of the mapping function $\Psi = \Psi(T,x,y,\varepsilon)$.

According to representation (2.4), the matrix A is equal to the product of the inverse mapping matrix $\boldsymbol{x} \to \boldsymbol{X}_0$ into the mapping matrix $\boldsymbol{x} \to \boldsymbol{X}$:

$$A = \Big(E - \frac{1}{2}\,I\,\frac{\partial^2\Psi}{\partial\boldsymbol{X}^2}\Big)^{-1}\Big(E + \frac{1}{2}\,I\,\frac{\partial^2\Psi}{\partial\boldsymbol{X}^2}\Big),$$

$$\frac{\partial^2\Psi}{\partial\boldsymbol{X}^2} = \begin{pmatrix} \Psi_{xx} & \Psi_{xy} \\ \Psi_{xy} & \Psi_{yy} \end{pmatrix}, \qquad I\,\frac{\partial^2\Psi}{\partial\boldsymbol{X}^2} = \begin{pmatrix} \Psi_{xy} & \Psi_{yy} \\ -\Psi_{xx} & -\Psi_{xy} \end{pmatrix}.$$

Using the identity

$$\Big(E - \frac{1}{2}\,I\,\frac{\partial^2\Psi}{\partial\boldsymbol{X}^2}\Big)^{-1} = \frac{1}{J}\Big(E + \frac{1}{2}\,I\,\frac{\partial^2\Psi}{\partial\boldsymbol{X}^2}\Big),$$

the matrix A can be represented as

$$A = \frac{1}{J}\left[(2-J)\begin{pmatrix} 1 & 0 \\ 0 & 1 \end{pmatrix} + \begin{pmatrix} \Psi_{xy} & \Psi_{yy} \\ -\Psi_{xx} & -\Psi_{xy} \end{pmatrix}\right], \tag{5.1}$$

where J is the Jacobian defined by (2.6).

Let us express the components of the local mapping matrix in terms of the second derivatives of the function Ψ and, for comparison, in terms of the second derivatives of the generating function, by writing this map in the form of (2.1):

$$\begin{gathered} A_{11} = \frac{2-J}{J} + \frac{\Psi_{xy}}{J} = \frac{(1+S_{XY})^2 - S_{XX}S_{YY}}{1+S_{XY}}, \\ A_{12} = \frac{\Psi_{yy}}{J} = \frac{S_{YY}}{1+S_{XY}}, \quad A_{21} = -\frac{\Psi_{xx}}{J} = -\frac{S_{XX}}{1+S_{XY}}, \quad A_{22} = \frac{2-J}{J} - \frac{\Psi_{xy}}{J} = \frac{1}{1+S_{XY}}. \end{gathered} \tag{5.2}$$

The map of a small neighborhood $(\delta X_0, \delta Y_0) \to (\delta X, \delta Y)$ with matrix A has two autonomous invariants under rotations of the coordinate system:

$$I_1 = A_{11} + A_{22}, \qquad I_2 = A_{12} - A_{21}.$$

For a parametric map, J and $\Delta\Psi = \Psi_{xx} + \Psi_{yy}$ are also invariants because they are expressed in terms of the invariants I_1 and I_2:

$$J = 4/(I_1+2), \qquad \Delta\Psi = 4I_2/(I_1+2).$$

Therefore, the condition $J > 0$ for the existence of a parametric map is invariant and can be represented as $I_1+2 > 0$. In contrast, the condition of existence of the map (2.2) with a generating function is noninvariant. In view of the last relation (5.2), the condition $J > 0$ can be represented as $A_{22} > 0$. Satisfaction of the inequality $A_{22} > 0$ depends on the choice of the coordinate system.

If a parametric map and the map (2.1) are calculated with the same asymptotic accuracy, the region of existence of the parametric map is much wider than the region of existence of the map (2.1). A more detailed comparison of these maps is given below.

In studies of transition to the random mode for two-dimensional maps, the invariant I_1 and the invariant $J(I_1)$, depending on the former, are of primary importance. The characteristic factor m is a root of the characteristic polynomial $m^2 - I_1 m + 1 = 0$ and depends only on I_1 or J.

It should be noted that in calculations of maps accurate to the third order by (4.2) in the degenerate case, the invariant J is determined from the formula (2.6) with accuracy up to the fifth order in ε. This makes it possible to accurately study the stability of a fixed point of the map and to describe transition to a random mode.

By the polar expansion theorem, known in analytic geometry, the matrix A is represented as the product of a rotation matrix and a symmetrical matrix. In turn, the symmetric matrix can be reduced to the principal axes by rotation of the coordinate system. Thus, we obtain

$$A = C(\varphi)C(\varphi_0)\begin{pmatrix} l_1 & 0 \\ 0 & l_2 \end{pmatrix} C(-\varphi_0), \quad l_1 l_2 = 1, \quad C(\varphi) = \begin{pmatrix} \cos\varphi & -\sin\varphi \\ \sin\varphi & \cos\varphi \end{pmatrix}. \tag{5.3}$$

The mapping $\delta\boldsymbol{X} = A\delta\boldsymbol{X}_0$ transforms a unit circle to an ellipse of the same surface area with axes l_1 and l_2. The angle φ_0 determines the direction of the fiber in the circle $|\delta\boldsymbol{X}_0| = 1$ that is elongated as much as possible by the mapping. The angle φ specifies the rotation of this fiber. Using (5.1) and (5.3), all the mapping characteristics listed above can be expressed in terms of elements of the Hessian matrix Ψ_{xx}, Ψ_{xy}, and Ψ_{yy}.

The largest and smallest elongations of the fiber are equal to

$$l_1 = R + \sqrt{R^2 - 1}, \quad l_2 = R - \sqrt{R^2 - 1}, \quad R^2 = ((2 - J)^2 + (\Psi_{xx} + \Psi_{yy})^2)/(4J^2) + 1/2.$$

The angles φ and φ_0 are given by

$$\tan\varphi = (A_{21} - A_{12})/(A_{11} + A_{22}), \quad \tan(\varphi + 2\varphi_0) = (A_{12} + A_{21})/(A_{11} - A_{22}).$$

The above-mentioned characteristics l_1, φ, m_1, and λ_1 are also invariants and expressed in terms of the two basic invariants. The angle φ_0 is not an invariant and depends on the choice of the coordinate axes δX and δY.

6. Advantages of the Parametric Mapping Method. In the parametric method, the function $\Psi(t, x, y)$ plays the role of a generating function. Just as in the generating function method, $\Psi(t, x, y)$ is determined from a Hamiltonian–Jacobi type equation.

However, as is noted above, the parametric method has a number of advantages over the generating function method:

1. Maps of simple form cannot be expressed in terms of a generating function. For example, rotation through 90° cannot be expressed in terms of $S(X_0, Y)$ (mapping $X = Y_0$, $Y = -X_0$). Using the function $\Psi = x^2 + y^2$ and formulas (2.8), these mapping is parametrized as follows:

$$X_0 = x - y, \quad Y_0 = y + x, \qquad X = x + y, \quad Y = y - x.$$

In this sense, the parametric representation is preferred.

2. Generally speaking, the resolvability condition (2.2) depends on the choice of Cartesian coordinates X and Y, whereas in the parametric method, the condition $J > 0$ is invariant under rotations of the coordinates X and Y.

3. In approximations of identical accuracy in the small parameter ε, the range of the parameter ε in which the condition $J > 0$ is satisfied is much wider than the range of ε in which the condition $1 + \partial^2 S/\partial X_0 \partial Y > 0$ is satisfied.

4. The coefficients Ψ_n of the series $\Psi = \varepsilon\Psi_1 + \varepsilon^2\Psi_2 + \ldots$ are much smaller than the coefficients of the series S_n for the generating function.

5. For an autonomous system, the function Ψ is represented as a series in odd powers of ε.

6. The map over time t and the averaged Hamiltonian are linked by the simple relation $\Psi = t\bar{H}(x, y)$ with accuracy up to ε^3.

The advantages of the parametric method will be shown for the case where the map is found exactly.

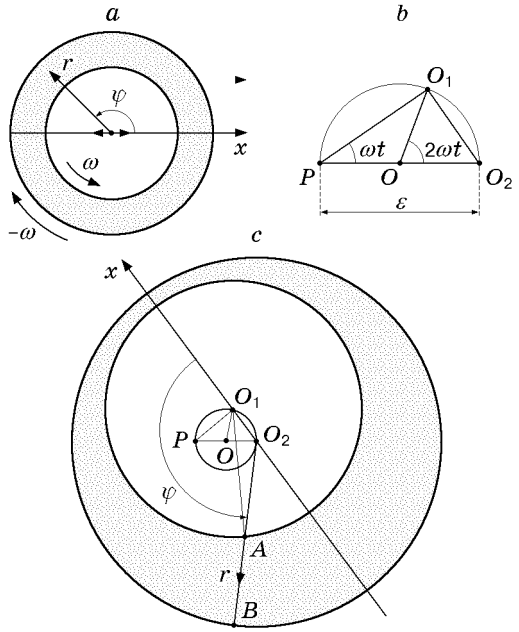

Fig. 1. Diagram of motion of the inner cylinder.

The Hamiltonian is given by

$$H = \varepsilon[(X^2 + Y^2)/2 + Xb\sin(t_0 + t)].$$

The system of equations is integrated exactly, and the coordinates X_n and Y_n of the recurrence points at times $t_n = 2\pi n$ are equal to

$$X_n - X_c = (X_{n-1} - X_c)\cos(2\pi\varepsilon) + (Y_{n-1} - Y_c)\sin(2\pi\varepsilon),$$

$$Y_n - Y_c = -(X_{n-1} - X_c)\sin(2\pi\varepsilon) + (Y_{n-1} - Y_c)\cos(2\pi\varepsilon),$$

$$X_c = [b\varepsilon^2/(1-\varepsilon^2)]\sin t_0, \qquad Y_c = [b\varepsilon/(1-\varepsilon^2)]\cos t_0.$$

The recurrence points lie on a circle with center X_c, Y_c, and the angular distance between them is equal to $2\pi\varepsilon$.

In the parametric method,

$$\Psi(x,y) = \tan(\pi\varepsilon)[(x - X_c)^2 + (y - Y_c)^2], \qquad J = 1/\cos^2(\pi\varepsilon) > 0.$$

In the generating function method,

$$S(X_0, Y) = [(1 - \cos(2\pi\varepsilon))/\cos(2\pi\varepsilon)](X_0 - X_c)(Y - Y_c) + \tan(2\pi\varepsilon)[(X_0 - X_c)^2 + (Y - Y_c)^2]/2,$$

$$1 + S_{XY} = 1/\cos(2\pi\varepsilon) > 0.$$

The example considered above leads to the following conclusions:

(a) the radii of convergence of the power series in ε for Ψ, equal to $1/\pi$, are twice the radii of convergence of the series for S (the parametric method allows rotations not exceeding 180°, and the method of generating functions allows rotations not exceeding 90°);

(b) The coefficient of the series Ψ_n is approximately a factor of 2^n smaller than the coefficient S_n; accordingly, for the remainders of these series r_n and R_n, the equality $r_n = 2^{-n}R_n$ holds.

Statements 1–6 are easily verified.

The example considered below is a rather complex nonintegrable hydrodynamic system of equations, in which transition to dynamic chaos for rather large values of the parameter ε can be described by the parametric method.

7. Unsteady Flow of a Viscous Fluid Layer between Eccentrically Rotating Cylinders. *Kinematics of Motion of Circular Cylinders.* We consider the motion a circular cylinder located inside another immovable

circular cylinder. The axes of both cylinders are vertical. Figure 1 gives a cross section of the cylinders, showing the region between two circles. The outer circle and its center O_2 are immovable. The inner circle rotates with angular velocity 2ω, so that the center of the inner circumference O_1 describes a circumference with fixed center O and radius $\varepsilon/2$. The angle O_1OO_2 varies as $\angle O_1OO_2 = 2\omega t$. In the rectangular triangle O_2O_1P, $\angle O_1PO_2 = \omega t$, and, therefore, the distance between the center varies under the harmonic law $|O_1O_2| = \varepsilon \sin(\omega t)$ (Fig. 1b). The center line (x axis) is perpendicular to the leg O_1P and rotates with angular velocity ω. The cylinders move in a coordinate system with a fixed center line (Fig. 1a) so that the inner cylinder rotates with angular velocity ω, and its center oscillates under the law $x = |O_1O_2| = \varepsilon \sin(\omega t)$. The outer cylinder in this coordinate system rotates with velocity $-\omega$ in opposition to the direction of rotation of the inner cylinder.

Let the radius of the inner circle be equal to R, and the radius of the outer circle to $R+1$. We calculate the distance AB between the two circles for large value of R. For this, we apply the cosine rule to the triangle O_1O_2A (Fig. 1c):

$$|O_1O_2|^2 + |O_2A|^2 - 2|O_1O_2|\,|O_2A|\cos\varphi = |O_1A|^2.$$

Substituting $|O_1O_2| = \varepsilon \sin(\omega t)$, $|O_1A| = R$, and $|O_2A| = R+1-|AB|$, we obtain the following equation for $|AB|$:

$$\varepsilon^2 \sin^2(\omega t) + (R+1-|AB|)^2 - 2\varepsilon \sin(\omega t)(R+1-|AB|)\cos\varphi = R^2.$$

From this we have

$$|AB| = 1 - \varepsilon \sin(\omega t)\cos\varphi + O(1/R). \tag{7.1}$$

Stream Function. We proceed to solving the problem of viscous incompressible flow in the layer between two cylinders. This problem was exactly solved by Petrov for the case of coaxial rotation. In the thin layer approximation ($R \gg 1$), Sommerfeld (1904) obtained a solution for the case where the inner cylinder rotates about its center and its center does not coincide with the center of the outer cylinder. Joukowski and Chaplygin solved this problem in the inertialess Stokes approximation without assuming this layer to be thin. The results were published in 1887 and 1906 [18]. In all the cases considered, the flow region does not vary with time, the flow is steady, and the stream function does not depend on time. In these cases, the equations of motion for the fluid particles form an integrable system. The fluid particles move along streamlines, on which the stream function is constant. Dynamic chaos is absent in such systems.

In our case, the flow region varies with time, the problem is substantially unsteady, and the stream function (Hamiltonian H) depends on time. To solve this problem, we shall use the asymptotic approximation $R \gg 1$ of lubricating layer theory. This approach was described in [19].

We shall seek the stream function in the form of the dependence $RH(t, \varphi, Y)$, where $Y = R+1-r$, and the velocity components in the form

$$v_\varphi = R\dot{\varphi} = R\,\frac{\partial H}{\partial Y}, \qquad v_Y = \dot{Y} = -\frac{\partial H}{\partial \varphi}, \tag{7.2}$$

where r and φ are polar coordinates with origin at the point O_2. In the variables φ and Y, the flow region is $\varphi \in (0, 2\pi)$, $Y \in (0, Y_{\max})$ and the upper boundary of the region is specified by Eq. (7.1):

$$Y_{\max} = |AB| = 1 - \varepsilon \sin(\omega t)\cos\varphi.$$

The motions of the fluid at $R \gg 1$ are given by the equations

$$\frac{\partial p}{\partial Y} = 0, \qquad \frac{\partial p}{R\partial \varphi} = \mu\,\frac{\partial^2 v_\varphi}{\partial Y^2}.$$

From this it follows that the pressure p depends only on the angle φ. Replacing the component v_φ by its expression in terms of the stream function, we obtain the equation

$$\frac{dp(\varphi)}{Rd\varphi} = \mu R\,\frac{\partial^3 v_\varphi}{\partial Y^3}. \tag{7.3}$$

The attachment conditions are satisfied on the boundaries of the cylinders:

$$Y = 0: \qquad H = 0, \quad \frac{\partial H}{\partial Y} = -\omega; \tag{7.4}$$

$$Y = Y_{\max}: \qquad -\frac{\partial H}{\partial \varphi} = \frac{\partial Y_{\max}}{\partial t} + \omega\,\frac{\partial Y_{\max}}{\partial \varphi}, \quad \frac{\partial H}{\partial Y} = \omega. \tag{7.5}$$

In addition, it is necessary to require that the pressure function $p(0) = p(2\pi)$ be unique. By virtue of (7.3), this condition is written as

$$\int_0^{2\pi} \frac{\partial^3 H}{\partial Y^3}\, d\varphi = 0. \tag{7.6}$$

The boundary-value problem (7.3)–(7.6) is solved as follows. Introducing the discharge function $Q(t,\varphi) = H(t,\varphi,Y_{\max})$, we represent the solution as

$$H = Q(t,\varphi)(3\tilde{Y}^2 - 2\tilde{Y}^3) + \omega Y_{\max}[-\tilde{Y}(1-\tilde{Y})^2 + \tilde{Y}^2(-1+\tilde{Y})], \quad \tilde{Y} = Y/Y_{\max}.$$

In this representation, the stream function satisfies Eq. (7.3), the boundary conditions (7.4), and the second condition (7.5). Substituting the expression for H into the first condition (7.5), we obtain the equation of conservation of mass in the layer:

$$\frac{\partial Q}{\partial \varphi} + \frac{\partial Y_{\max}}{\partial t} = 0.$$

Integrating this equation, we obtain $Q = \varepsilon\omega\cos(\omega t)\sin\varphi + c(t)$. From the uniqueness condition for pressure, we have $c(t) = 0$.

Thus, in the thin layer approximation, the Hamiltonian of the system has the form

$$H(t,\varphi,Y) = \omega\varepsilon\cos(\omega t)\sin\varphi(3\tilde{Y}^2 - 2\tilde{Y}^3) + \omega(\tilde{Y} - \tilde{Y}^2)Y_{\max}. \tag{7.7}$$

8. Motion of Viscous Fluid Particles between Eccentrically Rotating Cylinders. The positions of the Poincaré recurrence points φ_n and Y_n at times $t_n = 2\pi n/\omega$ are found by solving the Cauchy problem for the Hamiltonian equations (7.2):

$$\dot{\varphi} = \frac{\partial H}{\partial Y}, \quad \dot{Y} = -\frac{\partial H}{\partial \varphi}, \qquad \varphi(0) = \varphi_0, \quad Y(0) = Y_0. \tag{8.1}$$

At these times, the axis O_1 and O_2 of the inner and outer cylinders coincide, and the flow region in the variables φ and Y is a rectangle $\varphi \in [0, 2\pi)$, $Y \in (0,1)$. Figure 2 shows the Poincaré recurrence points for different values of the parameter ε, found by numerical solution of Eqs. (8.1) using the Runge–Kutta method. The points correspond to the times $t_n = 2\pi n/\omega$, $n = 0, 1, \ldots, 400$ at which the centers of the circles O_1 and O_2 coincide. In Fig. 2, the initial Poincaré recurrence points are denoted by filled circles and the fixed points by open circles. For $\varepsilon = 0$, the fluid flow is a simple shear Couette flow, and the points move along straight lines $Y = \text{const}$ (in polar coordinates, these are concentric circles). Even for small values of ε, the phase pattern is complicated and there is transition to chaos, which is generated at the point $\varphi = \pi$, $Y = 1/2$. It should be noted that the largest area of the chaotic region is reached at $\varepsilon = 0.5$. For $\varepsilon > 0.5$, two subregions with invariant curves of recurrence points grow at the center of the flow region as ε increases. The recurrence points that entered these subregions do not leave them. Thus, the best mixing is reached for $\varepsilon = 0.5$.

9. Poincaré Map. To reduce the Hamiltonian (7.7) to the standard form, we make two canonical replacements, using generating functions.

The first replacement $\varphi, Y \to \tilde{q}, \tilde{p}$, which maps a flow region with curvilinear boundaries $\varphi \in [0, 2\pi)$, $Y \in (0, Y_{\max})$ onto a rectangle $\tilde{q} \in [0, 2\pi)$, $\tilde{p} \in (-1/2, 1/2)$, corresponds to the generating function

$$S_1(\varphi,\tilde{p}) = \Big(\frac{1}{2} + \tilde{p}\Big)\int_0^{\varphi} Y_{\max}\, d\varphi = \Big(\frac{1}{2} + \tilde{p}\Big)(\varphi - \varepsilon\sin(\omega t)\sin\varphi).$$

Using the well-known formulas [11], we obtain

$$\tilde{q} = \frac{\partial S_1}{\partial \tilde{p}} = \varphi - \varepsilon\sin(\omega t)\sin\varphi, \qquad Y = \frac{\partial S_1}{\partial \varphi} = \Big(\frac{1}{2} + \tilde{p}\Big)Y_{\max} \tag{9.1}$$

and the Hamiltonian in the new variables:

$$\tilde{H}(t,\tilde{q},\tilde{p}) = \frac{\partial S_1}{\partial t} + H = -\omega\tilde{p}^2 + \varepsilon\omega\Big(\tilde{p}^2 - \frac{1}{4}\Big)(\sin(\omega t)\cos\varphi - 2\tilde{p}\cos(\omega t)\sin\varphi).$$

Here the dependence $\varphi(t,\tilde{q})$ is defined by the first of Eqs. (9.1).

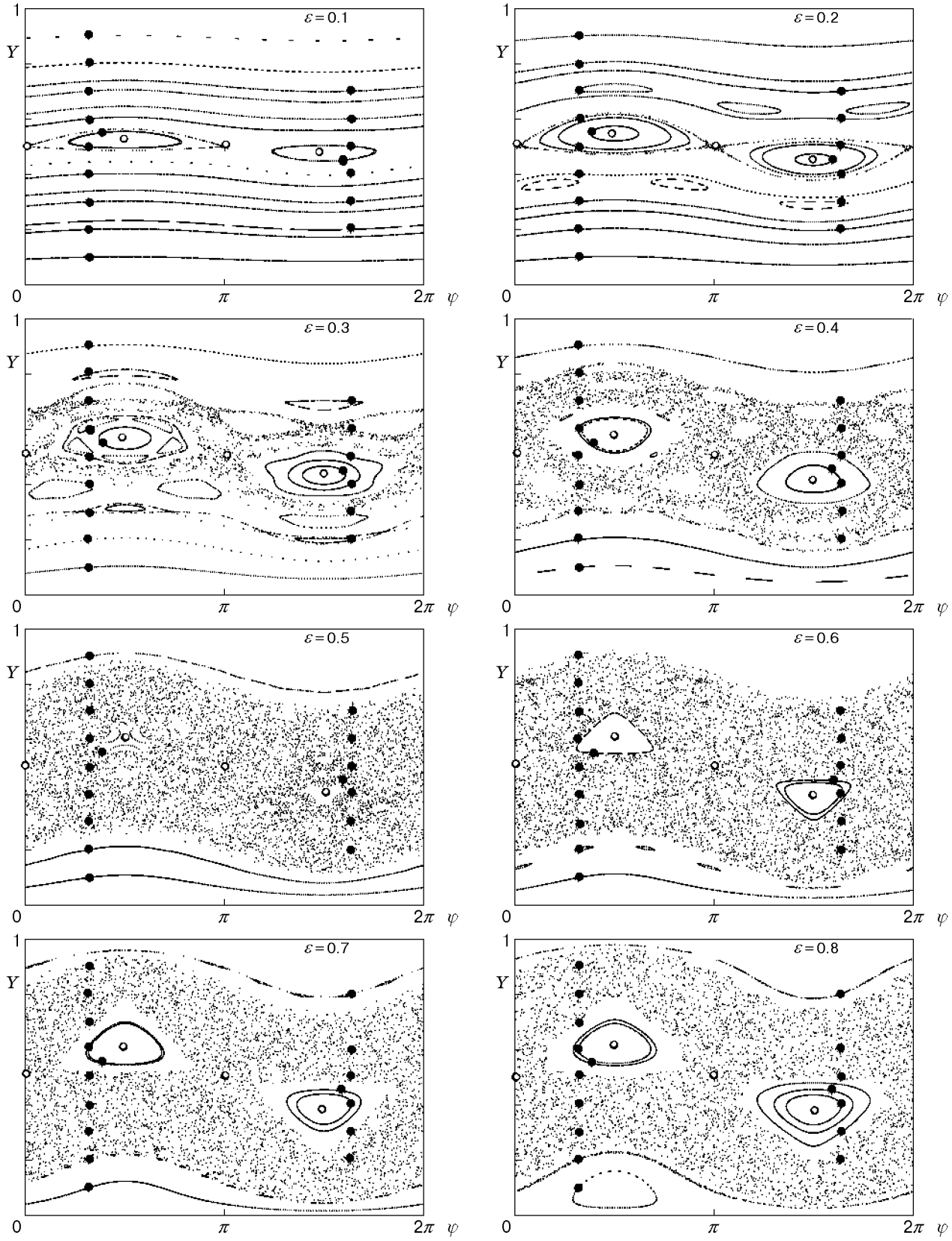

Fig. 2. Diagram of viscous flow between eccentrically rotating cylinders [numerical calculation by Eqs. (8.1) using the Runge–Kutta method]: filled circles are the initial Poincaré recurrence points and open circles are fixed points.

The second canonical replacement $\tilde{q}, \tilde{p} \to q, p$, which brings the system to the standard form, corresponds to the generating function $S_2(t, q, \tilde{p}) = \omega t \tilde{p}^2 - q\tilde{p}$. The formulas of change of variables and the modified Hamiltonian are written as

$$\tilde{q} = -\frac{\partial S_2}{\partial \tilde{p}} = q - 2p\omega t, \qquad p = -\frac{\partial S_2}{\partial q} = \tilde{p},$$
$$\tilde{\tilde{H}}(t, q, p) = \varepsilon\omega F(t, \varphi, p), \qquad F = (p^2 - 1/4)(\sin(\omega t)\cos\varphi - 2p\cos(\omega t)\sin\varphi). \tag{9.2}$$

Here φ, as a function of t, q, and p, is determined implicitly from the equation

$$\varphi - \varepsilon\sin(\omega t)\sin\varphi = q - 2p\omega t. \tag{9.3}$$

The equations of particle motion in the variables q and p are written as

$$\dot{q} = \frac{\partial \tilde{\tilde{H}}}{\partial p} = \varepsilon\omega\Big(\frac{\partial F}{\partial p} - \frac{2\omega t}{Y_{\max}}\,\frac{\partial F}{\partial \varphi}\Big), \qquad \dot{p} = -\frac{\varepsilon\omega}{Y_{\max}}\,\frac{\partial F}{\partial \varphi}. \tag{9.4}$$

From (9.3) we find the partial derivatives

$$\frac{\partial\varphi}{\partial t} = \frac{-2p\omega + \varepsilon\omega\cos(\omega t)\sin\varphi}{Y_{\max}}, \quad \frac{\partial\varphi}{\partial q} = \frac{1}{Y_{\max}}, \quad \frac{\partial\varphi}{\partial p} = -\frac{2\omega t}{Y_{\max}}$$

and the total derivative

$$\dot{\varphi} = \frac{\partial\varphi}{\partial t} + \dot{q}\,\frac{\partial\varphi}{\partial q} + \dot{p}\,\frac{\partial\varphi}{\partial p}.$$

Using the formulas for the derivative, we write the equations of particle motion (9.4) in the initial variables φ and Y:

$$\frac{d\varphi}{d\omega t} = -2p - 6\,\frac{\varepsilon}{Y_{\max}}\Big(p^2 - \frac{1}{4}\Big)\cos(\omega t)\sin\varphi,$$
$$\frac{dp}{d\omega t} = \frac{\varepsilon}{Y_{\max}}\Big(p^2 - \frac{1}{4}\Big)(\sin(\omega t)\sin\varphi + 2p\cos(\omega t)\cos\varphi), \tag{9.5}$$
$$Y = (1/2 + p)Y_{\max}.$$

The obtained system is equivalent to the initial system (8.1). PRP can be found numerically from this system. The result is identical to that obtained above.

Poincaré mapping makes it possible to calculate PRP from recursive relations. Using the parametric method described above, we construct the Poincaré map with accuracy up to ε^3. For this, we shall expand the Hamiltonian (9.2) as

$$\tilde{\tilde{H}}(\tau, q, p) = \varepsilon\omega H_1 + \varepsilon^2\omega H_2 + O(\varepsilon^3),$$

where

$$H_1 = (p^2 - 1/4)(\sin\tau\cos(q - 2p\tau) - 2p\cos\tau\sin(q - 2p\tau)),$$
$$H_2 = -(p^2 - 1/4)[\sin^2\tau\sin^2(q - 2p\tau) + (1/2)p\sin 2\tau\sin(2(q - 2p\tau))] \quad (\tau = \omega t),$$

and employ formula (4.2).

To simplify the calculations, we introduce the function

$$g(\tau, q, p) = \cos q - \cos\tau\cos(q - 2p\tau).$$

Then,

$$\int_0^{2\pi} H_1\,d\tau = \Big(p^2 - \frac{1}{4}\Big)g(\tau, q, p).$$

For the first approximation, we obtain

$$\Psi_1(q, p) = (p^2 - 1/4)g(2\pi, q, p) = -2f(p)\sin Q,$$
$$f(p) = (p^2 - 1/4)\sin(2\pi p), \qquad Q = q - 2\pi p.$$

For the second approximation,

$$\Psi_2(q,p) = \Psi_{21}(q,p) + \Psi_{22}(q,p),$$
$$\Psi_{21}(q,p) = -\frac{1}{2}\int\limits_0^{2\pi}\Big\{H_1, \int\limits_0^{\tau} H_1\, d\tau'\Big\}\, d\tau, \qquad \Psi_{22}(q,p) = \int\limits_0^{2\pi} H_2\, d\tau. \tag{9.6}$$

Using the identities

$$-\Big\{H_1, \int\limits_0^{\tau} H_1\, d\tau'\Big\} = \Big(p^2 - \frac{1}{4}\Big)^2 (g_{\tau q} g_p - g_{\tau p} g_q) + 2p\Big(p^2 - \frac{1}{4}\Big)(g_{\tau q} g - g_\tau g_q),$$

$$g_{\tau q} g_p - g_{\tau p} g_q = -2\sin q\, \frac{d}{d\tau}\,(\tau \cos\tau \sin Q) + 2(\cos\tau \sin Q)^2,$$

$$\int\limits_0^{2\pi} (g_{\tau q} g_p - g_{\tau p} g_q)\, d\tau = \pi(1 - 2\cos(4\pi p)) + \Big(2\pi - \frac{\sin(4\pi p)}{4p}\,\frac{8p^2-1}{4p^2-1}\Big)\cos 2Q,$$

$$\int\limits_0^{2\pi} (g_{\tau q} g - g_\tau g_q)\, d\tau = 2\pi p - \sin(4\pi p)$$

we find the integrals in (9.6) and the function Ψ for the Poincaré map:

$$\Psi(q,p) = \varepsilon\Psi_1(Q,p) + \varepsilon^2\Psi_2(Q,p) + O(\varepsilon^3), \quad \Psi_2(Q,p) = u(p) + v(p)\cos 2Q,$$
$$u(p) = \pi(p^2 - 1/4)^2(5/2 - \cos(4\pi p)) - p(p^2 - 1/4)\sin(4\pi p),$$
$$v(p) = \pi(p^2 - 1/4)^2 - (p^2 - 1/4)(p^2 - 5/8)\sin(4\pi p)/(4p).$$

Using (2.4), we obtain the Poincaré map

$$q_0 = x - \Psi_y/2, \quad p_0 = y + \Psi_x/2, \qquad q_1 = x + \psi_y/2, \quad p_1 = y - \psi_x/2, \tag{9.7}$$

which allows the coordinates of the next Poincaré recurrence point q_1 and p_1 to be calculated from the coordinates of the previous point q_0 and p_0. The initial coordinates of the PRP are found from the formulas $\varphi_0 = q_0$ and $\varphi_1 = q_1 - 4\pi p_1$.

The map (9.7) can be simplified by converting to the new variables $Q_0 = q_0 - 2\pi p_0$, $Q_1 = q_1 - 2\pi p_1$, and $x' = x - 2\pi y$:

$$Q_0 = x' - \Psi_y/2, \quad p_0 = y + \Psi_{x'}/2, \qquad Q_1 = x' + \Psi_y/2, \quad p_1 = y - \Psi_{x'}/2. \tag{9.8}$$

Then,

$$\Psi(x',y) = \varepsilon\Psi_1(x',y) + \varepsilon^2\Psi_2(x',y) + O(\varepsilon^3),$$
$$\Psi_1(x',y) = -2f(y)\sin x', \qquad \Psi_2(x',y) = u(y) + v(y)\cos 2x'. \tag{9.9}$$

Thus, the required Poincaré map $\varphi_0, Y_0 \to \varphi_1, Y_1$ is represented as a superposition of three maps.

The first map $\varphi_0, Y_0 \to Q_0, p_0$ is obtained from the formulas

$$p_0 = Y_0 - 1/2, \qquad Q_0 = \varphi_0 - 2\pi p_0. \tag{9.10}$$

The second map $Q_0, p_0 \to Q_1, p_1$ is determined in parametric form from formulas (9.8) and (9.9). The third map $Q_1, p_1 \to \varphi_1, Y_1$ is determined as follows:

$$Y_1 = p_1 + 1/2, \qquad \varphi_1 = Q_1 - 2\pi p_1. \tag{9.11}$$

Figure 3 shows the phase portraits of PRP for $\varepsilon = 0.2$ and 0.4 obtained by solution of the algebraic equations (9.8)–(9.11). A comparison with the corresponding phase portraits in Fig. 2 shows that they coincide qualitatively. Moreover, the positions of the fixed points, denoted by light circles, and the elliptic (stable fixed) and hyperbolic (unstable fixed) points practically coincide. In Figs. 2 and 3, the regions of chaotic and ordered motions of the

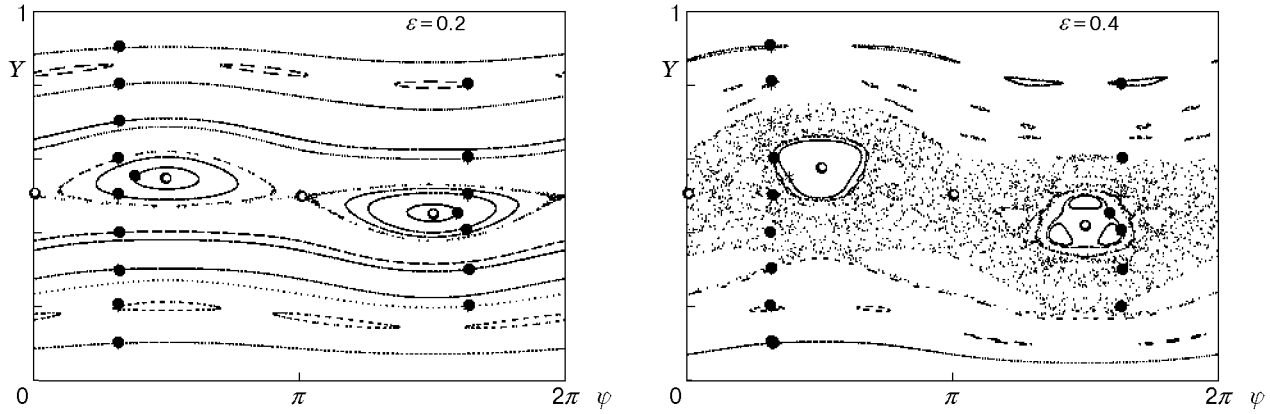

Fig. 3. Diagram of viscous flow between eccentrically rotating cylinders [asymptotic solution by Eqs. (9.8)–(9.11)]; notation same as in Fig. 2.

points differ little. Thus, for $\varepsilon < 0.5$, the accuracy of function (9.9) and the parametric map obtained using this function is sufficient to determine the phase trajectories of the PRP and to describe transition to chaos.

10. Fixed Points of the Poincaré Map. The phase portrait of PRP can be described qualitatively if one finds the fixed points of the map and study their stability. In the neighborhood of elliptic points, PRP lie on closed invariant curves similar to ellipses. Such motion is ordered.

In the neighborhood of hyperbolic points, PRP can be arranged randomly.

The fixed points can be found analytically using the map (9.8)–(9.11). The main fixed points are determined from the equations $Y_0 = Y_1$ and $\varphi_0 = \varphi_1$. From this, using (9.8)–(9.11), we obtain

$$p_0 = p_1 = y, \quad Y_0 = Y_1 = 1/2 + y, \quad \varphi_0 = \varphi_1 = x'; \tag{10.1}$$

$$\begin{gathered}\Psi_{x'} = -2\varepsilon \cos x'(f(y) + 2\varepsilon v(y) \sin x') = 0, \\ \Psi_y - 4\pi y = \varepsilon^2(u'(y) + v'(y) \cos 2x') - 2\varepsilon f'(y) \sin x' - 4\pi y = 0.\end{gathered} \tag{10.2}$$

System (10.2) is equivalent to the following two systems:

$$\cos x' = 0, \quad \varepsilon^2(u'(y) - v'(y)) - 2\varepsilon f'(y) \sin x' - 4\pi y = 0; \tag{10.3}$$

$$f(y) + 2\varepsilon v(y) \sin x' = 0, \quad \varepsilon^2(u'(y) + v'(y) \cos 2x') - 2\varepsilon f'(y) \sin x' - 4\pi y = 0. \tag{10.4}$$

System (10.3) has two roots, which can be obtained using asymptotic expansions in powers of y. The points corresponding to the roots

$$\begin{gathered}x' = \pi/2, \quad \varepsilon = 4y + 104y^3, \qquad y \in (0, 0.1), \\ x' = 3\pi/2, \quad \varepsilon = -4y - 104y^3, \qquad y \in (-0.1, 0)\end{gathered} \tag{10.5}$$

are denoted by M_1 and M_2. Using (10.1), from (10.5) we obtain the coordinates φ and Y of the points M_1 and M_2. For any values of ε, system (10.4) has two solutions:

$$x' = 0, \ y = 0, \qquad x' = \pi, \quad y = 0. \tag{10.6}$$

The points corresponding to these solutions are denoted by M_3 and M_4. In addition, for $\varepsilon > 0.587$, system (10.4) has solutions $\sin x' = -4.54y - 32.2y^3 + \ldots$ defined by the asymptotic series $\varepsilon = 0.587 + 17.7y^2 + \ldots$. However, for $\varepsilon > 0.5$, the obtained map is inapplicable, and, therefore, the last solutions are not considered. Thus, solution (10.6) defines two more fixed points M_3 and M_4. As follows from (10.1) and (10.6), the coordinates φ and Y of these points are equal to $(0, 1/2)$ and $(\pi, 1/2)$, respectively and do not depend on ε.

The obtained fixed points correspond to the periodic solutions of the Hamiltonian equations with a period $\omega t = 2\pi$. In addition, there are series of fixed points corresponding to a period of $2\pi n$. These points are determined from the equations $\varphi_n = \pi_0 + 2\pi k$ and $y_n = p_n - p_0$; they can also be found analytically. We shall restrict ourselves to consideration of the stability of the obtained fixed points (10.5) and (10.6).

In the neighborhood of a fixed point, we have

$$dQ_1 = A_{11}dQ_0 + A_{12}\,dp_0, \qquad dp_1 = A_{21}dQ_0 + A_{22}\,dp_0,$$

$$dQ_0 = d\varphi_0 - 2\pi\,dp_0, \qquad d\varphi_1 = dQ_1 - 2\pi\,dp_1,$$

where the coefficients A_{ij} [see (5.2)] are expressed in terms of the second derivatives of the parametric function $\Psi(x', y)$ defined by formula (9.9). The second group of equalities follows from (9.10) and (9.11). From these linear relations, we obtain

$$d\varphi_1 = \tilde{A}_{11}\,d\varphi_0 + \tilde{A}_{12}\,dp_0, \qquad dp_1 = \tilde{A}_{21}\,d\varphi_0 + \tilde{A}_{22}\,dp_0,$$

$$\tilde{A}_{11} = A_{11} - 2\pi A_{21}, \qquad \tilde{A}_{12} = A_{12} - 2\pi(A_{11} + A_{22}) + 4\pi^2 A_{21}, \tag{10.7}$$

$$\tilde{A}_{21} = A_{21}, \qquad \tilde{A}_{22} = A_{22} - 2\pi A_{21}.$$

The first invariant of the map (10.7) has the form

$$I = \tilde{A}_{11} + \tilde{A}_{22} = A_{11} + A_{22} - 4\pi A_{21}.$$

The matrix coefficients are expressed in terms of the function Ψ in (9.9) using formulas (5.2):

$$I = 2(2 - J)/J + 4\pi\Psi_{xx}/J. \tag{10.8}$$

The secular equation $m^2 - Im + 1 = 0$ for $|I| \leqslant 2$ has complex roots with absolute values equal to unity. In this case, the fixed points are stable (elliptic points). In view of (10.8), the stability conditions are written as

$$-1 \leqslant \pi\Psi_{x'x'} = 2\pi\varepsilon f(y)\sin x' - 4\pi\varepsilon^2 v(y)\cos 2x' \leqslant J - 1,$$
$$J - 1 = (\Psi_{xx}\Psi_{yy} - \Psi_{xy}^2)/4. \tag{10.9}$$

Let us study the stability of the fixed points M_1 and M_2 [see (10.5)]. Using the series $f(y) = -(\pi/2)y + (2\pi + \pi^3/3)y^3 + \ldots$, $v(y) = -(3/32)\pi + ((3/8)\pi + (5/12)\pi^3)y^2 + \ldots$, the condition (10.9) becomes $-1 \leqslant -10(\pi y)^2$. From this it follows that for $0 \leqslant y \leqslant y_0 \approx 1/(\pi\sqrt{10}) \approx 0.1$ and $\varepsilon \leqslant \varepsilon_0 \approx 0.505$, the point M_1 $[\pi/2, 1/2 + \varepsilon/4 + O(\varepsilon^3)]$ is stable. The second symmetrical fixed point M_2 $[3\pi/2, 1/2 - \varepsilon/4 + O(\varepsilon^3)]$ is stable for the same values of the parameter ε. These fixed points obtained in numerical experiments are shown by light circles in Fig. 2. For $\varepsilon = 0.1$, 0.2, 0.3, and 0.4, the points are elliptic points. In the neighborhood of these points, PRP are located on closed invariant curves. For $\varepsilon = 0.5$, the fixed points M_1 and M_2 lose stability, and the flow region is almost entirely filled chaotically with PRP.

The stability of the fixed points M_3 and M_4 [see (10.6)] is studied similarly. We calculate the second derivatives Ψ at these points:

$$\Psi_{xx} = -4\varepsilon^2 v(0) = 3\pi\varepsilon^2/8, \quad \Psi_{yy} = \varepsilon^2(u''(0) + v''(0)) = \varepsilon^2(5\pi/4 + 11\pi^3/6) = 60.8\varepsilon^2,$$

$$\Psi_{xy} = 2\varepsilon f'(0) = -\varepsilon\pi, \quad J - 1 = -2.467\varepsilon^2 + 17.9\varepsilon^4.$$

Substituting these derivatives into the stability condition, we obtain $-1 \leqslant 3.7\varepsilon^2 < -2.47\varepsilon^2 + 17.9\varepsilon^4$. From this it follows that the fixed points $M_3(0, 1/2)$ and $M_4(\pi, 1/2)$ are unstable for $\varepsilon < 0.587$, i.e., they are hyperbolic points. For $\varepsilon > 0.587$, these points are stable but the map (9.8)–(9.11) is inapplicable for $\varepsilon > 0.5$.

The numerical calculations agree with the theoretical conclusions. In Fig. 2, the fixed points M_3 and M_4 (open points) are hyperbolic points. For small ε, chaos occurs in small neighborhoods of these points. The areas of the chaotic regions increase with increase in ε. For $\varepsilon \approx 0.5$, the area of the chaotic region is maximal. In this case, all fixed points M_1, M_2, M_3, and M_4 are unstable.

Conclusions. The motion of viscous fluid particles between eccentrically rotating cylinders (see Fig. 1) is described by the Hamiltonian equations (9.5). For small eccentricity ($\varepsilon \leqslant 0.2$), the PRP are located on invariant curves (see Fig. 2) and chaos is not observed. The Poincaré map over the period has four fixed points (see Fig. 2): elliptic points M_1 $(\pi/2, 1/2 + \varepsilon/4)$ and M_2 $(3\pi/2, 1/2 - \varepsilon/4)$ for $\varepsilon < 0.5$ and hyperbolic points M_3 $(0, 1/2)$ and M_4 $(\pi, 1/2)$ for any ε. In the neighborhood of the hyperbolic points, dynamic chaos is observed for $\varepsilon > 0.2$. The area of the chaotic region of the PRP increases as ε increases to the value $\varepsilon \approx 0.5$. For $\varepsilon = \varepsilon_0 \approx 0.5$, the points M_1 and M_2 become hyperbolic in a small time interval $\Delta\varepsilon$. At this moment, the area of the chaotic region is maximal.

For $\varepsilon > \varepsilon_0 + \Delta\varepsilon$, the points M_1 and M_2 become elliptic again. In the neighborhood of these points, the motion is ordered, and the area of the chaotic region decreases, accordingly.

The Poincaré parametric mapping is an effective tool for calculating fixed points, studying their stability, and describing transition to chaos. The phase portraits of PRP obtained by the calculated Poincaré map are in good agreement with results of numerical experiments (see Fig. 3).

The example considered is a mathematical model of a mixer for mixing high-viscosity media. The best mixing is attained at $\varepsilon \approx 0.5$.

We thank D. M. Klimov and V. F. Zhuravlev for useful discussions of the results of this work.

This work was supported by the Russian Foundation for Fundamental Research (Grant No. 02-01-00567).

REFERENCES

1. G. M. Zaslavskii, *Stochasticity of Dynamic Systems* [in Russian], Nauka, Moscow (1983).
2. A. Lichtenberg and M. Lieberman, *Regular and Stochastic Motion*, Springer, Heidelberg (1982).
3. *Trans. of the Inst. of Eng. on Electronics and Radioelectronics*, Vol. 75, No. 8, Random Systems (1987).
4. G. Shuster, *The Deterministic Chaos*, Physic-Verlag, Weinheim (1984).
5. N. N. Bogolyubov and Yu. A. Mitropo'lskii, *Asymptotic Methods in the Theory of Nonlinear Oscillations* [in Russian], Nauka, Moscow (1974).
6. V. F. Zhuravlev and D. M. Klimov, *Applied Methods in Oscillation Theory* [in Russian], Nauka, Moscow (1988).
7. A. I. Neishtadt, "Separation of motions in systems with a rapidly rotating phase," *Prikl. Mat. Mekh.*, **48**, No. 3, 197–204 (1984).
8. J. M. Ottino, *The Kinematics of Mixing: Stretching, Chaos, and Transport*, Cambridge Univ. Press, Cambridge (1989).
9. R. M. Kronover, *Fractals and Chaos in Dynamical Systems. Fundamentals of Theory* [in Russian], Postmarked, Moscow (2000).
10. A. G. Petrov, "Motion of particles of an incompressible medium in a region with a periodically varying boundary," *Izv. Akad. Nauk SSSR, Mekh. Zhidk. Gaza*, No. 4, 12–17 (2000).
11. V. F. Zhuravlev, *Fundamentals of Theoretical Mechanics* [in Russian], Nauka, Fizmatlit, Moscow, (1997).
12. V. I. Arnol'd, *Mathematical Methods of Classical Mechanics* [in Russina], Éditorial URRS, Moscow (2000).
13. R. Courant and D. Hilbert, *Methods of Mathematical Physics, Interscience*, Vol. 2, New York (1953).
14. G. E. O. Giacaglja, *Perturbation Methods in Non-Linear Systems*, New York (1972).
15. A. G. Petrov, "Averaging Hamiltonian systems," *Izv. Ross. Akad. Nauk., Mekh. Tverd. Tela*, No. 3, 19–33 (2001).
16. A. G. Petrov, "Averaging Hamiltonian systems with a time periodic Hamiltonian," *Dokl. Ross. Akad. Nauk*, **368**, No. 4, 483–488 (1999).
17. L. I. Sedov, "*Mechanics of Continuous Media*" [in Russian], Vol. 1, Nauka, Moscow (1970).
18. N. E. Joukowski, *Complete Collected Papers*, Vol. 3: *Hydraulics. Applied Mechanics* [in Russian], Gostekhteoretizdat, Leningrad–Moscow (1949), pp. 121–133.
19. N. E. Kochin, I. A. Kibel', and N. V. Roze, *Theoretical Fluid Mechanics* [in Russian], Part 2, Fizmatgiz, Moscow (1963).